Crystal structure of bisoprolol fumarate Form I, $(C_{18}H_{32}NO_4)$ $(C_4H_2O_4)_{0.5}$

James A. Kaduk,[1,2,a] Amy M. Gindhart,[3] and Thomas N. Blanton[3]
[1]*Illinois Institute of Technology, 3101 S. Dearborn St., Chicago, Illinois 60616, USA*
[2]*North Central College, 131 S. Loomis St., Naperville, Illinois 60540, USA*
[3]*ICDD, 12 Campus Blvd., Newtown Square, Pennsylvania 19073-3273, USA*

(Received 6 June 2019; accepted 26 August 2019)

The crystal structure of bisoprolol fumarate Form I has been solved and refined using synchrotron X-ray powder diffraction data and optimized using density functional techniques. Bisoprolol fumarate Form I crystallizes in space group *P*-1 (#2) with $a = 8.165\ 70(5)$ Å, $b = 8.516\ 39(12)$ Å, $c = 16.751\ 79(18)$ Å, $\alpha = 89.142(1)°$, $\beta = 78.155(1)°$, $\gamma = 81.763(1)°$, $V = 1128.265(10)$ Å^3, and $Z = 2$. The neutral side chain of the bisoprolol cation is probably disordered. The cation and anion are linked by N–H···O and O–H···O hydrogen bonds. The cations are also linked by N–H···O hydrogen bonds. The result is alternating layers of hydrophilic and hydrophobic layers parallel to the *ab*-plane. The density of the structure is relatively low at 1.130 g cm^{-3}, but there are no obvious voids in the structure. The powder pattern is included in the Powder Diffraction File™ as entry 00-066-1625. © *2019 International Centre for Diffraction Data*. [doi:10.1017/S0885715619000757]

Key words: bisoprolol fumarate, Zebeta, powder diffraction, Rietveld refinement, density functional theory

I. INTRODUCTION

Bisoprolol fumarate (brand names Zebeta, Emcor, Isoten, and Seafuri) is a beta-blocker, one of a class of medicines used to treat cardiovascular diseases. Bisoprolol fumarate is prescribed for the treatment of hypertension, cardiac ischemia, congestive heart failure, and as a preventive treatment for heart attacks. The IUPAC name (CAS Registry number 104344-23-2) is (±)-1-(4-((2-(1-methylethoxy)ethoxy) methyl)phenoxy)-3((1-methylethyl)amino)-2-propanol(*E*)-2-butenedioate (2:1 salt). A two-dimensional molecular diagram of bisoprolol fumarate is shown in Figure 1.

Powder diffraction data for Forms I and II of bisoprolol fumarate, as well as that for a hydrate, are reported in Detrich et al. (2018). A peak list for Form I is also reported in Chinese Patent Application CN10634909A (Wang *et al.*, 2016).

This work was carried out as part of a project (Kaduk *et al.*, 2014) to determine the crystal structures of large-volume commercial pharmaceuticals and include high-quality powder diffraction data for these pharmaceuticals in the Powder Diffraction File (Fawcett *et al.*, 2017).

II. EXPERIMENTAL

Bisoprolol fumarate was a commercial reagent, USP Lot #G0D316, and was used as-received. The white powder was packed into a 1.5 mm diameter Kapton capillary and rotated during the measurement at ~50 Hz. The powder diffraction pattern was measured at 295 K at beamline 11-BM (Lee *et al.*, 2008; Wang *et al.*, 2008) of the Advanced Photon Source at Argonne National Laboratory using a wavelength of 0.413 342 Å from 0.5° to 50° 2θ with a step size of 0.001° and a counting time of 0.1 s step^{-1}. A laboratory powder diffraction pattern of a second sample (USP Lot #R01980) (measured on a PANalytical Empyrean diffractometer equipped with an incident-beam focusing mirror and an X'Celerator detector, from 1° to 50° 2θ in 0.016 7113 steps, 4 s step^{-1}, 1/4° divergence slit, 0.02 radian Soller slits, rotated 0.7 mm glass capillary using Mo$K\alpha$ radiation) was similar to the synchrotron diffraction pattern (Figure 2), confirming that the material is replicable.

The pattern was indexed on a primitive triclinic unit cell with $a = 8.1622$ Å, $b = 8.5281$ Å, $c = 16.7484$ Å, $\alpha = 89.107°$, $\beta = 78.178°$, $\gamma = 81.728°$, $V = 1129.1$ Å^3, and $Z = 2$ using N-TREOR (Altomare *et al.*, 2013). Since this compound is sold as a racemate, the space group was assumed to be $P-1$, which was confirmed by the successful solution and refinement of the structure. A reduced cell search in the Cambridge Structural Database (Groom *et al.*, 2016) combined with the chemistry C, H, N, and O only yielded no hits. A connectivity search on bisoprolol likewise yielded no hits. A bisoprolol cation and a fumarate dianion were built using Spartan '16 (Wavefunction, 2017) and saved as mol2 files. The saved mol2 files were converted into MOPAC files using OpenBabel (O'Boyle *et al.*, 2011). Many attempts to solve the structure using multiple programs were unsuccessful. The structure was finally solved by Monte Carlo simulated annealing using EXPO2014 (Altomare *et al.*, 2013). A bisoprolol cation and half of a fumarate dianion were used as fragments. One of the ten solutions yielded a better fit than the others. There were N–H···O hydrogen bonds between the bisoprolol and the fumarate, but the C56–C56 double bond across the center of symmetry at the center of the fumarate was 2.37 Å, much longer than the expected value of 1.31 Å.

The structure was refined GSAS (Toby, 2001; Larson and Von Dreele, 2004). For reasons that are as yet unclear,

[a]Author to whom correspondence should be addressed. Electronic mail: kaduk@polycrystallography.com

https://doi.org/10.1017/S0885715619000757 Published online by Cambridge University Press

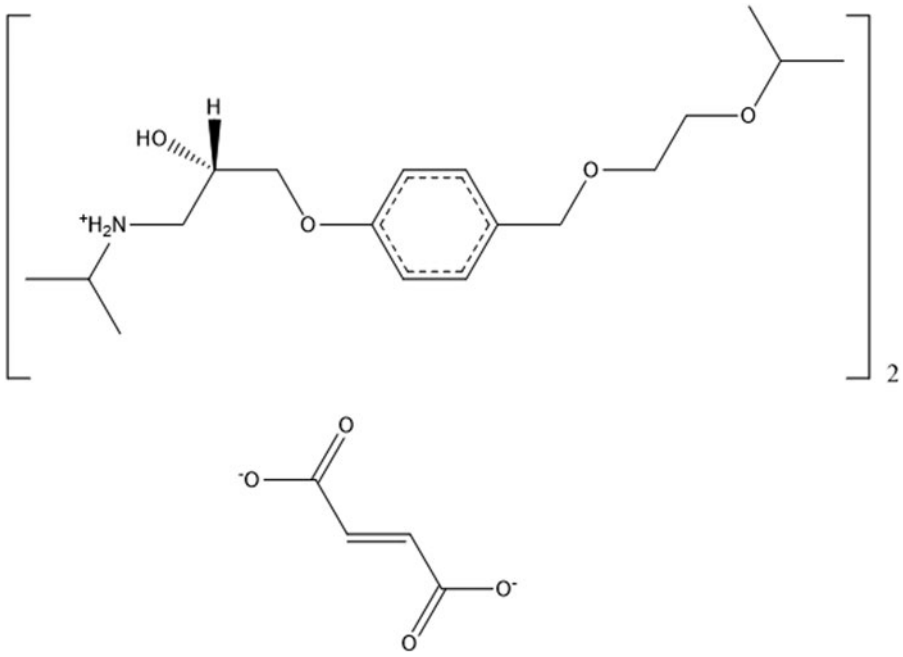

Figure 1. Molecular structure of bisoprolol fumarate.

attempts to refine the structure using GSAS-II failed. Only the 1.0–22.0° 2θ portion of the pattern was included in the refinement (d_{min} = 1.083 Å). All non-H bond distances and angles were subjected to restraints, based on a Mercury/Mogul Geometry Check (Bruno *et al.*, 2004; Sykes *et al.*, 2011) of the molecule. The Mogul average and standard deviation for each quantity were used as the restraint parameters. The C56–C56 double bond between the two halves of the fumarate dianion was restrained to 1.31(3) Å. The restraints contributed 8.7% to the final χ^2. The U_{iso} of the non-H atoms were grouped by chemical similarity. The U_{iso} of each hydrogen atom was fixed at 1.3× that of the heavy atom to which it was attached. The peak profiles were described using the profile function #4 (Thompson *et al.*, 1987; Finger *et al.*, 1994), which includes the Stephens (1999) anisotropic strain broadening model. The background was modeled using a three-term shifted Chebyshev polynomial, with a six-term diffuse scattering function to model the Kapton capillary and any amorphous component. The initial refinement (even with restraints) yielded large displacement coefficients in the neutral side chain C35–C52 and a chemically unreasonable topology. The refinement was re-started

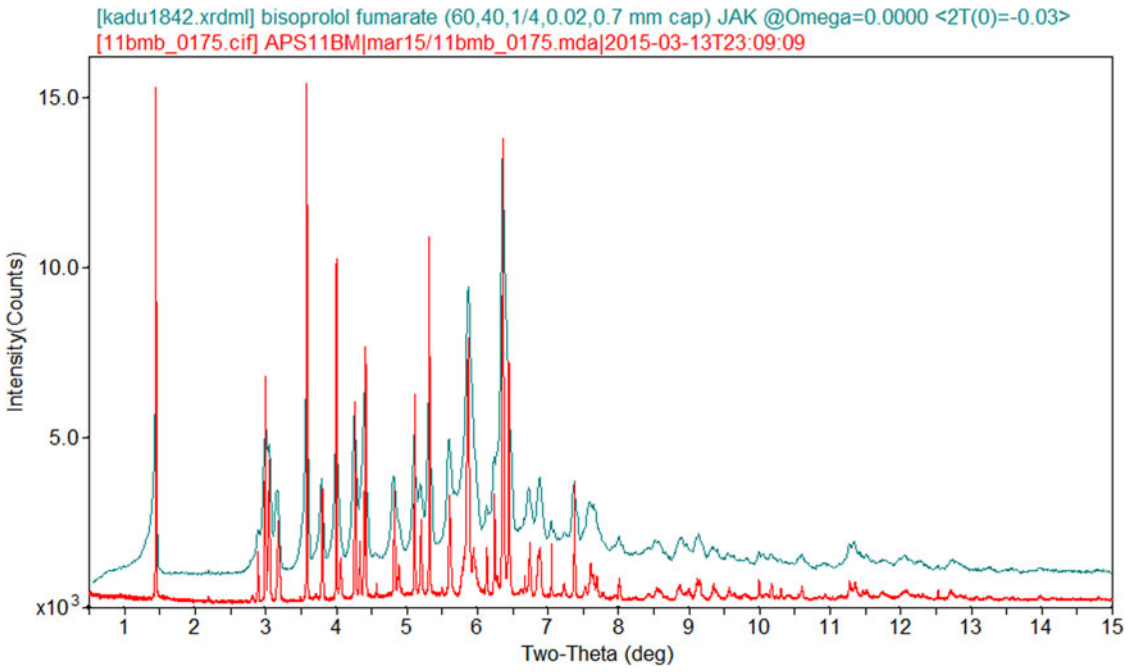

Figure 2. Comparison of the synchrotron and laboratory (Mo$K\alpha$) powder diffraction data on bisoprolol fumarate. The laboratory data were converted to the synchrotron wavelength of 0.413 342 Å using Jade 9.8 (MDI, 2017).

https://doi.org/10.1017/S0885715619000757 Published online by Cambridge University Press

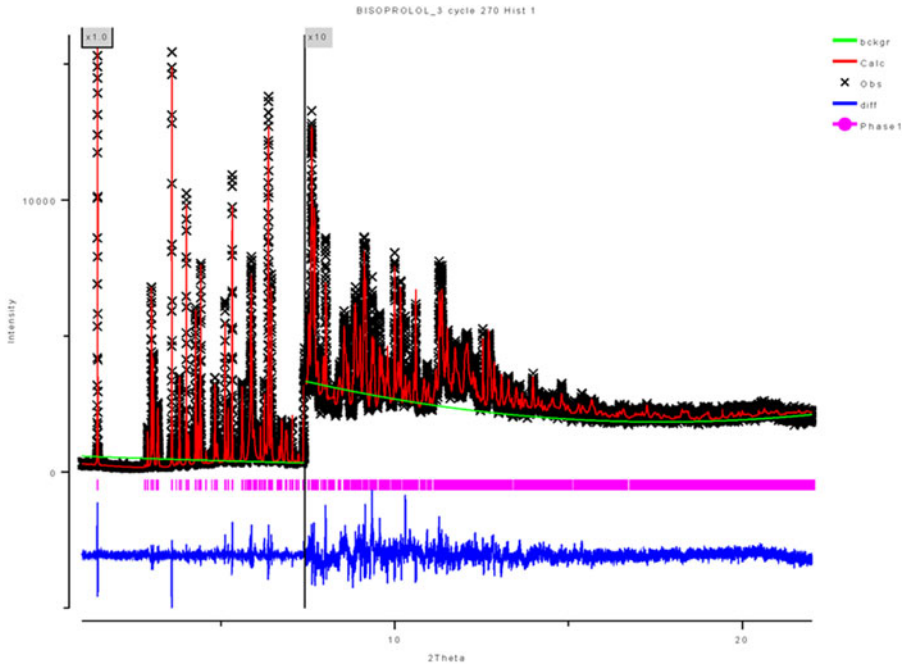

Figure 3. Rietveld plot for the synchrotron pattern refinement of bisoprolol fumarate. The black crosses represent the observed data points, and the red line is the calculated pattern. The blue curve is the difference plot, plotted at the same scale as the other patterns. The vertical scale has been multiplied by a factor of 10 for $2\theta > 7.4°$.

from the result of the density functional theory (DFT) calculation. The final refinement of 131 variables using 21 060 observations (21 002 data points and 58 restraints) yielded the residuals $R_{wp} = 0.054$, $R_p = 0.0701$, and $\chi^2 = 2.909$. The largest peak (1.00 Å from C19) and hole (1.88 Å from C52) in the difference Fourier map were 0.40 and -0.46 eÅ^{-3}, respectively. The Rietveld plot is included in Figure 3. The largest errors in the fit are in the positions and shapes of some of the low-angle peaks and may reflect subtle specimen damage.

The structure was also refined using the laboratory data with GSAS-II (Toby and Von Dreele, 2013), using a similar strategy as with the synchrotron data, except that the data did not support the refinement of the generalized strain broadening model. The final refinement of 109 variables using 1706 observations and 59 restraints yielded the residuals $R_{wp} =$ 0.0715 and GOF = 4.51. The largest peak and hole in the difference Fourier map were 0.27 and $-0.24(6)$ eÅ^{-3}, respectively. The Rietveld plot is included in Figure 4. A peak at 9.79° 2θ indicates that an unidentified impurity phase is

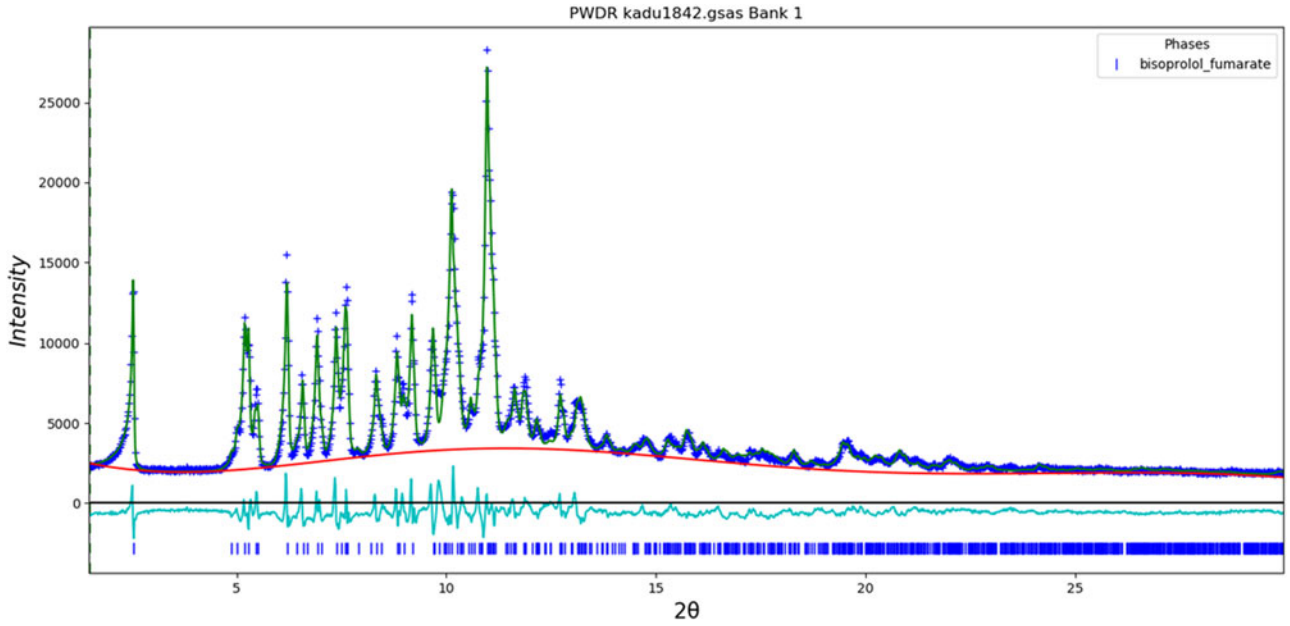

Figure 4. Rietveld plot for the laboratory pattern refinement of bisoprolol fumarate. Intensity is plotted on a square root scale. The blue crosses represent the observed data points, and the green line is the calculated pattern. The red line is the background, which included the diffuse scattering. The cyan curve is the difference pattern.

https://doi.org/10.1017/S0885715619000757 Published online by Cambridge University Press

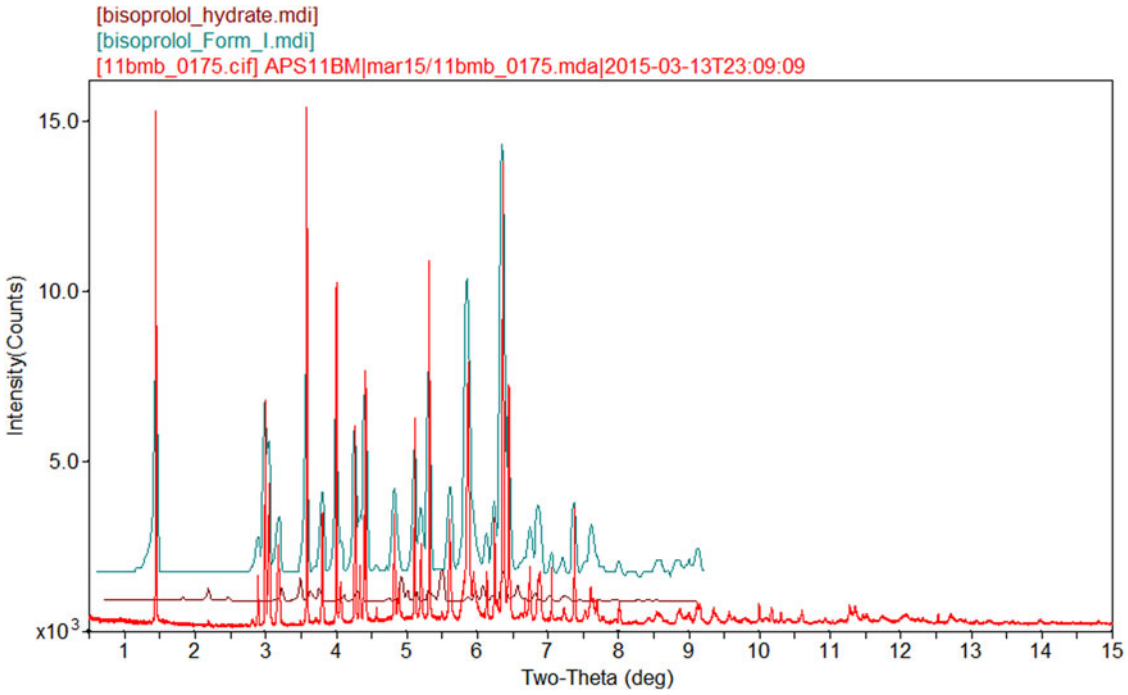

Figure 5. Comparison of the synchrotron pattern of bisoprolol fumarate with the pattern of Form I from Detrich *et al.* (2019), as well as that of bisoprolol hydrate. The literature patterns (measured using Cu$K\alpha$ radiation) were digitized using UN-SCAN-IT (Silk Scientific, 2013) and scaled to the synchrotron wavelength of 0.413 342 Å using Jade 9.8 (MDI, 2017).

present. This peak is not present in the synchrotron pattern, so it represents a sample-specific impurity.

A density functional geometry optimization (fixed experimental unit cell) was carried out using VASP (Kresse and Furthmüller, 1996) through the MedeA graphical interface (Materials Design, 2016). The calculation was carried out on 16 2.4 GHz processors (each with 4 GB RAM) of a 64-processor HP Proliant DL580 Generation 7 Linux cluster at North Central College. The calculation used the GGA-PBE functional, a plane wave cutoff energy of 400.0 eV, and a *k*-point spacing of 0.5 $Å^{-1}$ leading to a $2 \times 2 \times 1$ mesh, and took ~8 h. A density functional geometry optimization was also carried out using CRYSTAL14 (Dovesi *et al.*, 2014). The basis sets for the H, C, N, and O atoms were those of Gatti *et al.* (1994). The calculation was run on eight 2.1 GHz Xeon cores (each with 6 GB RAM) of a 304-core Dell Linux cluster at Illinois Institute of Technology, using eight *k*-points and the B3LYP functional, and took ~24 h.

III. RESULTS AND DISCUSSION

The powder pattern matches that of Form I from Detrich *et al.* (2019) (Figure 5) and Wang *et al.* (2016) (Figure 6) well enough to conclude that the material studied here is bisoprolol fumarate Form I. A trace of the bisoprolol hydrate form appears to be present in the synchrotron sample.

The root-mean-square (rms) Cartesian displacement between the non-H atoms of the cations in the synchrotron and laboratory structures is 0.443 Å (Figure 7), and the largest difference is 1.099 Å. The biggest differences are in the isopropyl group of the neutral side chain C35–C52, but there are many significant differences. The average precision of the C–C bonds in the synchrotron structure is 0.011 Å,

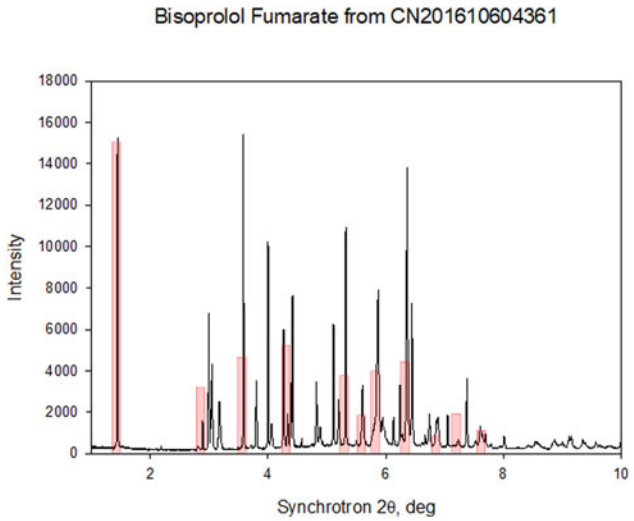

Figure 6. Comparison of the synchrotron pattern of bisoprolol fumarate (black) to the powder data reported in Wang *et al.* (2016) (pink bars).

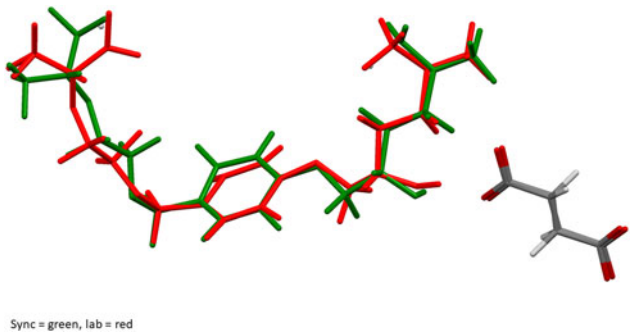

Figure 7. Comparison of the refined structures of bisoprolol fumarate using the synchrotron (green) and laboratory (red) data.

https://doi.org/10.1017/S0885715619000757 Published online by Cambridge University Press

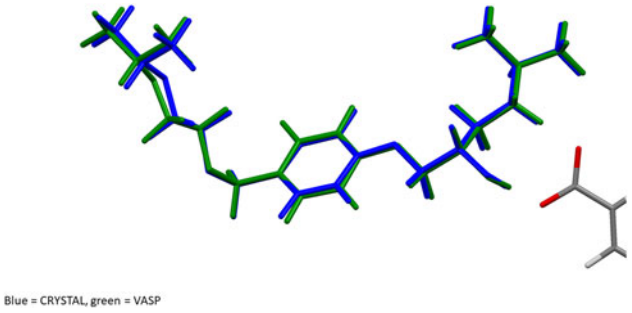

Figure 8. Comparison of the CRYSTAL14- (blue) and VASP-optimized (green) structures of the bisoprolol cation.

Figure 9. Comparison of the CRYSTAL14-optimized (blue) and Rietveld-refined (red) structures of the bisoprolol cation.

while that in the laboratory structure is 0.069 Å; the laboratory structure is much less precise than the synchrotron structure.

The refined atom coordinates of bisoprolol fumarate and the coordinates from the DFT optimizations are reported in the CIFs attached in Supplementary Material. The rms Cartesian displacement between the CRYSTAL and VASP structures is 0.212 Å (Figure 8). The largest differences are in the neutral side chain. This discussion will concentrate on the synchrotron and CRYSTAL14 structures. Comparing the Rietveld-refined and optimized structures, the rms Cartesian displacements of the non-H atoms in the bisoprolol cation are 0.787 Å (Figure 9). The largest differences are in the neutral side chain. Removing these atoms from the overlay decreases the rms displacement to 0.483 Å. The agreement between the refined and optimized structures is outside of the normal range for correct structures (van de Streek and Neumann, 2014), but the general nature of the structure seems to be correct. The asymmetric unit (with the atom numbering) is illustrated in Figure 10, and the crystal structure is presented in Figures 11 and 12. The U_{iso} of the atoms in the neutral side chain are much larger than those in other parts of the structures, suggesting that this chain may be disordered. These "flexible" regions lie next to each other in the structure and away from the more rigid hydrogen-bonded regions.

All of the bond distances and angles and almost all the torsion angles fall within the normal ranges indicated by a Mercury/Mogul Geometry Check (Macrae *et al.*, 2008). The torsion angles C12–O11–C4–C2 and O45–C42–C39–O38 are flagged as unusual. The value of 28° for C12–O11–C4–C2 lies on the tail of a bimodal 0/180° distribution of similar torsion angles. The value of 174° for O45–C42–C39–O38 lies in a minor *trans* population of a mainly ±*gauche* distribution of similar torsion angles.

Quantum chemical geometry optimization (DFT/B3LYP/6-31G*/water) using Spartan '16 (Wavefunction, 2017) indicated that the observed conformation of the bisoprolol cation is 9.1 kcal mol^{-1} higher in energy than the local minimum. The geometry differences span the whole molecule but are largest in the cationic side chain. Molecular mechanics conformational analysis indicated that the observed conformation is 4.9 kcal mol^{-1} higher in energy than the global minimum-energy conformation, but that the general shapes of the molecules are similar. These energy differences indicate that cation–anion interactions are significant in determining the molecular conformation.

Analysis of the contributions to the total crystal energy using the Forcite module of Materials Studio (Dassault, 2017) suggests that bond and angle distortion terms are the most significant contributions to the intramolecular deformation energy, but that they are relatively small. The intermolecular energy is dominated by electrostatic attractions, which in this force-field-based analysis include hydrogen bonds. The hydrogen bonds are better analyzed using the results of the DFT calculation.

Hydrogen bonds are prominent in the crystal structure (Table I). The cation and anion are linked by N22–H24···O and O17–H18···O59 hydrogen bonds. The result of these is a ring with a graph set (Etter, 1990; Bernstein *et al.*, 1995; Shields *et al.*, 2000) *R*2,2(9). The cations are linked by N22–H23···O17 hydrogen bonds. The result is a complex chain of hydrogen bonds roughly along the 320 axis. The

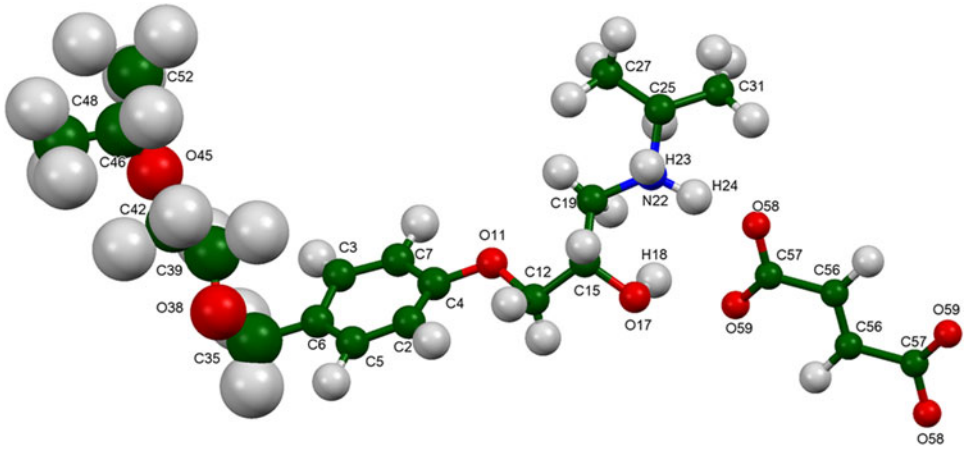

Figure 10. Molecular structure of bisoprolol fumarate, with the atom numbering. The atoms are represented by 50% probability spheroids.

https://doi.org/10.1017/S0885715619000757 Published online by Cambridge University Press

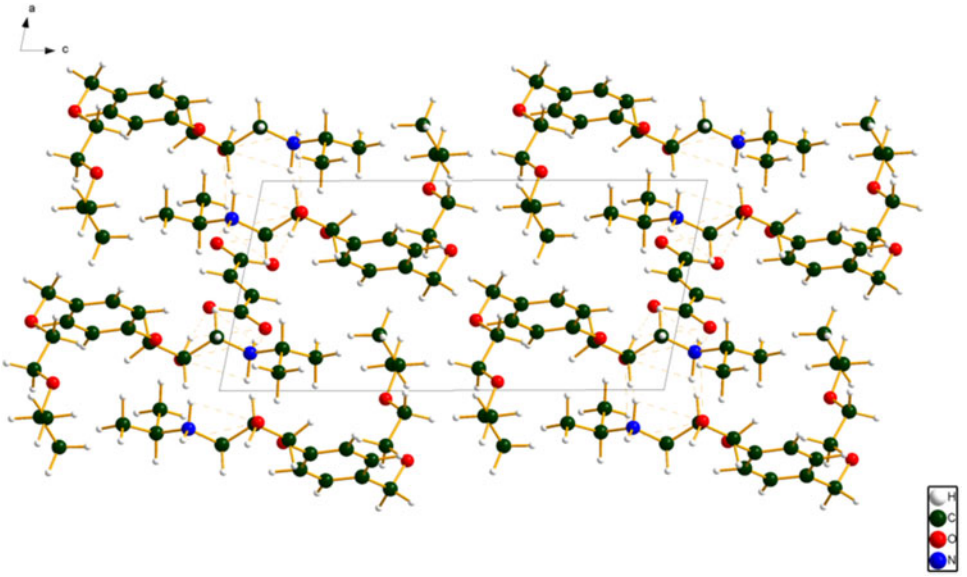

Figure 11. Crystal structure of bisoprolol fumarate, viewed down the *b*-axis.

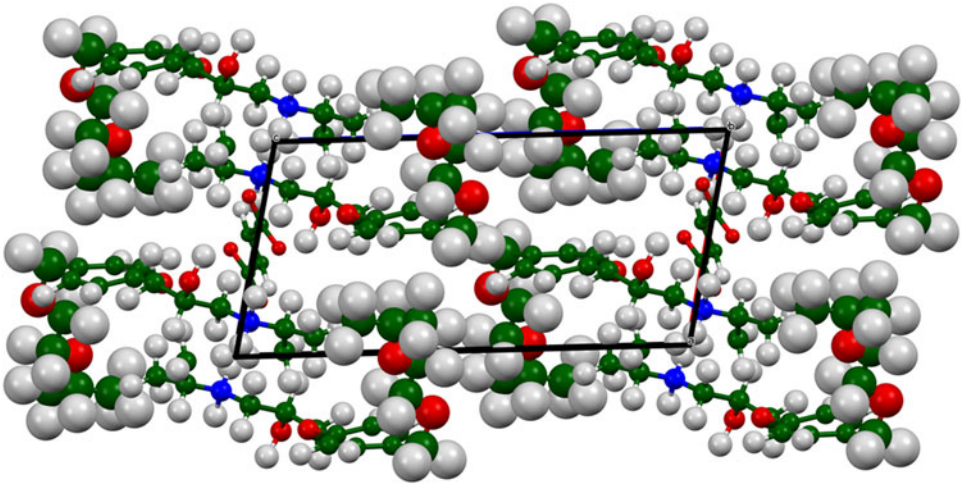

Figure 12. Crystal structure of bisoprolol fumarate, viewed down the *b*-axis, and including the thermal ellipsoids.

TABLE I. Hydrogen bonds (CRYSTAL14) in bisoprolol fumarate.

H-bond	D–H (Å)	H···A (Å)	D···A (Å)	D–H···A (°)	Overlap (*e*)	*E* (kcal mol^{-1})
N22–H23···O17	1.041	1.810	2.798	157.0	0.072	6.2
N22–H24···O58	1.068	1.645	2.711	174.4	0.101	7.3
O17–H18···O59	1.003	1.641	2.635	169.8	0.075	15.0
C46–H47···O38	1.100	2.794	3.710	140.5	0.012	
C31–H33···O17	1.094	2.685	3.437	125.5	0.010	
C15–H16···O58	1.098	2.619	3.621	151.4	0.015	
C7–H9···O59	1.084	2.158	3.155	151.9	0.031	
C2–H1···O45	1.082	2.156	3.181	157.0	0.028	
C39–H41···C6	1.099	2.722[a]	3.068		0.011	
H40···H36		2.438[a]			0.011	

[a]Intramolecular.

energies of the N–H···O hydrogen bonds were calculated by the correlation of Wheatley and Kaduk (2018), and that of the O–H···O hydrogen bonds was calculated by the correlation of Rammohan and Kaduk (2018). The crystal structure is characterized by alternation hydrophilic and hydrophobic layers parallel to the *ab*-plane. Several C–H···O hydrogen bonds contribute to the crystal energy. Visually, hydrophobic–hydrophobic interactions seem to take place, but there is only weak evidence for them in the Mulliken population analysis.

A calculation of the Connolly surface (probe radius = 1.2 Å) using Materials Studio (Dassault, 2017) indicated that the free

https://doi.org/10.1017/S0885715619000757 Published online by Cambridge University Press

volume was 3.8%. A void calculation in Mercury using the same radius yielded no voids. The volume/non-H atom is 20.9 $Å^3$. The calculated density is 1.130 g cm^{-3}.

The Bravais–Friedel–Donnay–Harker (Bravais, 1866; Friedel, 1907; Donnay and Harker, 1937) morphology suggests that we might expect platy morphology for bisoprolol fumarate, with {001} as the principal faces. A fourth-order spherical harmonic preferred orientation model was included in both the synchrotron and laboratory refinements. The texture indices were 1.12 and 1.20, respectively, so preferred orientation was significant in these rotated capillary specimens. The powder pattern of bisoprolol fumarate from this synchrotron data set is included in the Powder Diffraction File™ as entry 00-066-1625.

SUPPLEMENTARY MATERIAL

The supplementary material for this article can be found at https://doi.org/10.1017/S0885715619000757.

ACKNOWLEDGEMENTS

We thank Lynn Ribaud and Saul Lapidus for their assistance in the data collection and Andrey Rogachev for the use of computing resources at IIT.

FUNDING INFORMATION

Use of the Advanced Photon Source at Argonne National Laboratory was supported by the U. S. Department of Energy, Office of Science, Office of Basic Energy Sciences, under Contract No. DE-AC02-06CH11357. This work was partially supported by the International Centre for Diffraction Data.

CONFLICTS OF INTEREST

The authors have no conflicts of interest to declare.

Altomare, A., Cuocci, C., Giacovazzo, C., Moliterni, A., Rizzi, R., Corriero, N., and Falcicchio, A. (**2013**). "EXPO2013: a kit of tools for phasing crystal structures from powder data," J. Appl. Crystallogr. **46**, 1231–1235.

Bernstein, J., Davis, R. E., Shimoni, L., and Chang, N. L. (**1995**). "Patterns in hydrogen bonding: functionality and graph set analysis in crystals," Angew. Chem. Int. Ed. Engl. **34**(15), 1555–1573.

Bravais, A. (**1866**). *Etudes Cristallographiques* (Gauthier Villars, Paris).

Bruno, I. J., Cole, J. C., Kessler, M., Luo, J., Motherwell, W. D. S., Purkis, L. H., Smith, B. R., Taylor, R., Cooper, R. I., Harris, S. E., and Orpen, A. G. (**2004**). "Retrieval of crystallographically-derived molecular geometry information," J. Chem. Inf. Sci. **44**, 2133–2144.

Dassault Systèmes (**2017**). *Materials Studio 2018* (BIOVIA, San Diego, CA).

Detrich, A., Dömötör, K. J., Kagtona, M. T., Markovits, I., and Láng, J. V. (**2018**). "Polymorphic forms of bisoprolol fumarate," J. Therm. Anal. Calorim. **135**, 3043–3055.

Donnay, J. D. H. and Harker, D. (**1937**). "A new law of crystal morphology extending the law of Bravais," Am. Mineral. **22**, 446–447.

Dovesi, R., Orlando, R., Erba, A., Zicovich-Wilson, C. M., Civalleri, B., Casassa, S., Maschio, L., Ferrabone, M., De La Pierre, M., D-Arco, P., Noël, Y., Causà, M., and Kirtman, B. (**2014**). "CRYSTAL14: a program for the *ab initio* investigation of crystalline solids," Int. J. Quantum Chem. **114**(19), 1287–1317.

Etter, M. C. (**1990**). "Encoding and decoding hydrogen-bond patterns of organic compounds," Acc. Chem. Res. **23**(4), 120–126.

Fawcett, T. G., Kabekkodu, S. N., Blanton, J. R., and Blanton, T. N. (**2017**). "Chemical analysis by diffraction: the Powder Diffraction File™," Powder Diffr. **32**(2), 63–71.

Finger, L. W., Cox, D. E., and Jephcoat, A. P. (**1994**). "A correction for powder diffraction peak asymmetry due to axial divergence," J. Appl. Crystallogr. **27**(6), 892–900.

Friedel, G. (**1907**). "Etudes sur la loi de Bravais," Bull. Soc. Fr. Mineral. **30**, 326–455.

Gatti, C., Saunders, V. R., and Roetti, C. (**1994**). "Crystal-field effects on the topological properties of the electron-density in molecular crystals - the case of urea," J. Chem. Phys. **101**, 10686–10696.

Groom, C. R., Bruno, I. J., Lightfoot, M. P., and Ward, S. C. (**2016**). "The Cambridge Structural Database," Acta Crystallogr. Sect. B: Struct. Sci., Cryst. Eng. Mater. **72**, 171–179.

Kaduk, J. A., Crowder, C. E., Zhong, K., Fawcett, T. G., and Suchomel, M. R. (**2014**). "Crystal structure of atomoxetine hydrochloride (Strattera), $C_{17}H_{22}NOCl$," Powder Diffr. **29**(3), 269–273.

Kresse, G. and Furthmüller, J. (**1996**). "Efficiency of ab-initio total energy calculations for metals and semiconductors using a plane-wave basis set," Comput. Mater. Sci. **6**, 15–50.

Larson, A. C. and Von Dreele, R. B. (**2004**). "General Structure Analysis System (GSAS)," Los Alamos National Laboratory Technical Report LAUR 86–784.

Lee, P. L., Shu, D., Ramanathan, M., Preissner, C., Wang, J., Beno, M. A., Von Dreele, R. B., Ribaud, L., Kurtz, C., Antao, S. M., Jiao, X., and Toby, B. H. (**2008**). "A twelve-analyzer detector system for high-resolution powder diffraction," J. Synchrotron Radiat. **15**(5), 427–432.

Macrae, C. F., Bruno, I. J., Chisholm, J. A., Edington, P. R., McCabe, P., Pidcock, E., Rodriguez-Monge, L., Taylor, R., van de Streek, J., and Wood, P. A. (**2008**). "Mercury CSD 2.0 – new features for the visualization and investigation of crystal structures," J. Appl. Crystallogr. **41**, 466–470.

Materials Design (**2016**). *MedeA 2.20.4* (Materials Design Inc., Angel Fire, NM).

MDI (**2017**). *Jade 9.8* (Materials Data. Inc., Livermore, CA).

O'Boyle, N., Banck, M., James, C. A., Morley, C., Vandermeersch, T., and Hutchison, G. R. (**2011**). "Open Babel: an open chemical toolbox," J. Chem. Inform. **3**, 33.

Rammohan, A. and Kaduk, J. A. (**2018**). "Crystal structures of alkali metal (Group 1) citrate salts," Acta Crystallogr. Sect. B: Struct. Sci., Cryst. Eng. Mater. **74**, 239–252.

Shields, G. P., Raithby, P. R., Allen, F. H., and Motherwell, W. S. (**2000**). "The assignment and validation of metal oxidation states in the Cambridge Structural Database," Acta Crystallogr. Sec. B: Struct. Sci. **56**(3), 455–465.

Silk Scientific (**2013**). *UN-SCAN-IT 7.0* (Silk Scientific Corporation, Orem, UT).

Stephens, P. W. (**1999**). "Phenomenological model of anisotropic peak broadening in powder diffraction," J. Appl. Crystallogr. **32**, 281–289.

Sykes, R. A., McCabe, P., Allen, F. H., Battle, G. M., Bruno, I. J., and Wood, P. A. (**2011**). "New software for statistical analysis of Cambridge Structural Database data," J. Appl. Crystallogr. **44**, 882–886.

Thompson, P., Cox, D. E., and Hastings, J. B. (**1987**). "Rietveld refinement of Debye-Scherrer synchrotron X-ray data from Al_2O_3," J. Appl. Crystallogr. **20**(2), 79–83.

Toby, B. H. (**2001**). "EXPGUI, a graphical user interface for GSAS," J. Appl. Crystallogr. **34**, 210–213.

Toby, B. H. and Von Dreele, R. B. (**2013**). "GSAS II: the genesis of a modern open source all purpose crystallography software package," J. Appl. Crystallogr. **46**, 544–549.

van de Streek, J. and Neumann, M. A. (**2014**). ""Validation of molecular crystal structures from powder diffraction data with dispersion-corrected density functional theory (DFT-D)," Acta Crystallogr. Sect. B: Struct. Sci., Cryst. Eng. Mater. **70**(6), 1020–1032.

Wang, J., Toby, B. H., Lee, P. L., Ribaud, L., Antao, S. M., Kurtz, C., Ramanathan, M., Von Dreele, R. B., and Beno, M. A. (**2008**). "A dedicated powder diffraction beamline at the Advanced Photon Source: commissioning and early operational results," Rev. Sci. Inst. **79**, 085105.

Wang, Y., Li, X., Lu, T., Peng, Y., and Fan, Y. (**2016**). "Bisoprolol fumarate I crystal form and preparation method thereof," Chinese Patent Application CN 10634909.

Wavefunction, Inc. (**2017**). *Spartan '16 Version 2.0.1* (Wavefunction Inc., Irvine, CA).

Wheatley, A. M. and Kaduk, J. A. (**2018**). "Crystal structures of ammonium citrates," Powder Diffr. **34**, 35–43.

https://doi.org/10.1017/S0885715619000757 Published online by Cambridge University Press